PROCEEDINGS OF SCIENCE

First result of a search for Diffuse Supernova Neutrino Background in SK-Gd experiment

M.Harada[a,*] **for the Super-Kamiokande collaboration**

[a] *Okayama University,*
700-8530 Okayama, Okayama, Japan

E-mail: pc3g4sej@s.okayama-u.ac.jp

Since 2020, Super-Kamiokande (SK) detector has been updated by loading gadolinium (Gd) as a new experimental phase, 'SK-Gd.' In the SK-Gd experiment, we can search low-energy electron antineutrinos via inverse-beta decay with efficient neutron identification thanks to high cross-section and high-energy gamma-ray emission of thermal neutron capture on Gd. Until July 2022, the observation is operated with the 0.01% Gd mass concentration. The neutron capture fraction on Gd is about 50% in this situation. In this paper, the first search result for the flux of astrophysical electron antineutrinos for the energy range of $O(10)$ MeV in SK-Gd with a 22.5×552 kton·day exposure at 0.01% Gd mass concentration of the initial stage of SK-Gd is reported.

38th International Cosmic Ray Conference (ICRC2023)
26 July - 3 August, 2023
Nagoya, Japan

*Speaker

PoS(ICRC2023)1173

1. Introduction

Neutrino emission is essential in the core-collapse supernova (CCSN) explosion. However, the neutrino observation from supernova has been successful only once so far due to the low probability of a CCSN occurring close enough to observe neutrinos. Therefore, the Diffuse Supernova Neutrino Background (DSNB) is eagerly tried to observe in the worldwide neutrino detector. DSNB is an integrated flux of neutrinos emitted from all past supernovae in the universe. This is also called Supernova Relic Neutrinos (SRNs).

The theoretical expectations for the DSNB flux depend on various parameters, such as the supernova rate introduced from the cosmic star formation rate, the neutrino mass ordering, the equations of states for the remnant, the metallicity of the galaxy, the failed supernova rate, and the binary interaction effect of stars.Therefore, the observation of DSNB would give us much variable information about not only the supernova explosion mechanism but also the star formation history in our universe.

One of the aims of the Super-Kamiokande (SK) experiment[1] is to observe DSNB. All types of neutrinos are emitted from CCSN and drive in the universe as DSNB. Among them, electron anti-neutrino has the largest cross-section via inverse beta decay (IBD) reaction ($\overline{\nu}_e + p \rightarrow e^+ + n$) in the energy range around few tens MeV. Thus, the previous search for DSNB in SK [2] is to identify the positron signal below 30 MeV and the following neutron signal due to the thermal neutron capture on the nucleus. This double coincidence event identification, called delayed coincidence, has the advantage of removing the background without following the neutron and lowering the energy threshold.

In the previous SK search, although the search couldn't observe the DSNB signal at that time, the world's stringent upper limit on the DSNB flux was placed above the 15.3 MeV region for the neutrino energy. At that time, a 2.2 MeV gamma ray from a thermal neutron capture reaction on a proton was used as a neutron signal. However, the neutron signal is very low energy for SK to be enough to detect, so the detection efficiency of the delayed neutron signal was about 20%.

The further reduction of background and the expansion of energy region in search is needed to observation of DSNB. Therefore, the new experimental phase called SK-Gd is proposed [3]. Gd has the largest cross-section for the thermal neutron capture among all stable elements. Also, the gamma rays emitted from the reaction are a total of $\sim$ 8 MeV, which can be enough to detect in SK. Therefore, SK-Gd enables to detection of neutron signals with high-detection efficiency by loading Gd in SK.

In July 2020, the first Gd loading to the SK tank was operated [4]. At this time, the Gd mass concentration is 0.011%, and it results in the neutron capture time constant of $\sim$ 115 μs. Figure 1 shows an illustration of the neutron signal by the neutron capture on the Gd in the SK-Gd experiment. To evaluate neutron detection in the SK-Gd experiment, a new neutron detection algorithm to identify the Gd signal [5] and the new detector simulation [6] based on Geant4 [7] was developed. At this time, we report a new search for the DSNB in the neutrino energy range of 9.3–31.3 MeV.

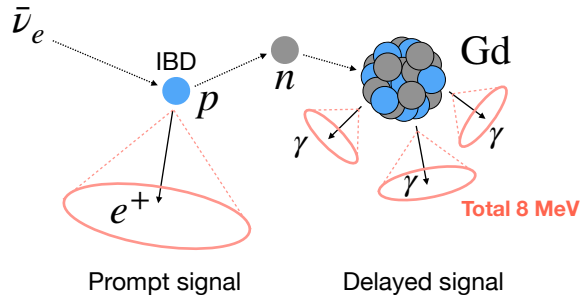

Figure 1: Illustration of the form of delayed neutron signal in the SK-Gd experiment.

2. Event selection

To search the DSNB signal, reductions of background events originating from various sources are required. The major background sources in the search energy region are atmospheric neutrino interaction events, the radioactive decay of isotopes originating from the spallation by cosmic-ray muons, and reactor neutrino events.

The atmospheric neutrino typically has a few hundred MeV. However, some of the charged-current and neutral-current interactions finally result in forming an event with a few tens MeV. The Charged-Current Quasi-Elastic (CCQE) reaction of neutrinos produces nucleons and charged lepton corresponding to the incoming neutrino flavor. In the case of electron (anti-electron) neutrinos, the produced lepton is electron (positron), and the lower energy tail component penetrates the signal region. If the neutrinos are muon type, the produced muon sometimes has lower energy than the muon Cherenkov threshold. In that case, the muon doesn't emit any photons, and it becomes invisible (invisible muon), and only electrons produced muon decay is detected. The event has a well-known Michel spectrum, and these have components in the signal energy region. On the other hand, the Neutral-Current Quasi-Elastic (NCQE) reaction knocks out nucleons and makes an excitation state to the remaining nucleus. The nucleus emits deexcitation gamma rays, and these become background. Because the nuclei knocked out from the nucleus sometimes cause secondary interaction with other nuclei and results in multiple gamma-ray emission, the energy spectrum of the NCQE background has large uncertainty.

SK is exposed by the 2 Hz of cosmic-ray muons. The radioactive isotope decay originating from the spallation by the cosmic-ray muon (muon spallation background) is dominant below 16 MeV. These events are difficult to link to the parent muon because the lifetime is typically larger than the SK event window. Especially, the events from the decay of ^{9}Li (Li9) remain in the final background because the decay has the $\beta + n$ channel with 51%, a long-live time of 0.26 s, and a relatively high yield (1.9×10^{-7} μ^{-1} g^{-1} cm^2) [8]. The production rate of the Li9 event in SK is measured to be 0.86 ± 0.12 (stat.) ± 0.15 (syst.) kton$^{-1} \cdot$ day^{-1} [9], and a prediction of the spectrum of β is given in [2].

If the electron or positron events, which do not have any neutrons, which are misidentified as neutrons, accidentally form the pair of delayed coincidences, these are inevitable backgrounds. Other spallation events than the Li9 event dominantly contribute to this background because the

spallation event rate is about $O(10^6)$ times higher than the DSNB signals. To extract the meaningful search result over the background, the spallation event reduction is required to be $O(10^{-6})$ reduction by combining with lowering the neutron misidentification probability.

Because the reactor neutrinos consist of electron antineutrinos, the background events are the IBD and are completely the same as DSNB. However, the energy of these events is typically lower than the search energy range. Thus, the events do not have so much effect on the search. The event selection basically the same method as the previous DSNB search [2] is applied to the prompt positron event. The search neutrino energy range corresponds to the positron kinetic energy range of 7.5–29.5 MeV. At this time, the major background of this search, such as a radioactive isotope decays originating from muon spallation, atmospheric neutrino events, and other backgrounds from detector originating, are removed. In addition, neutron tagging, which is an event selection using the following neutron, is applied. The number of delayed neutrons signal in the IBD event search is definitely one. Therefore, the prompt events with exactly one delayed neutron signal are selected as the IBD event. The spallation event can be reduced to $O(1)\%$ by the reduction. Thus, the misidentification probability of neutron is required to reduce it to $O(10^{-4})$ per event in order to remove accidental coincidence background events. To achieve such a low probability, the additional neutron selection cut criteria, which are above 3.5 MeV, are applied in the neutron selection. By applying this cut, the neutron identification efficiency is estimated to be $35.6 \pm 2.5\%$, and the misidentification probability is found to be $(2.8 \pm 0.2) \times 10^{-4}$ per event.

Figure 2 shows the total signal efficiency for IBD events between 7.5–29.5 MeV in the positron kinetic energy. The efficiency is evaluated for each 2 MeV energy bin. Above 15.5 MeV, the signal efficiency by spallation cut is reduced due to applying harsher spallation cut to ensure the spallation background to a negligible level. Final signal efficiency, shown as the red line, is about twice larger than the previous search [2], especially below 15.5 MeV thanks to the higher neutron detection efficiency.

3. Search Result

A series of data reductions are applied to the observed data taken in 552.2 days of live time in the initial period of the SK-Gd experiment. As a result, 16 events remain in the signal energy region. Figure 3 shows the comparison of reconstructed kinetic energy spectra between observed data and the expected background. The signal energy region is separated into five energy bins by considering the kinds of backgrounds. The width of the first and second bins are 2 MeV, and these have enough statistics. The third bin is the largest energy, including Li9 and accidental background events. The fourth bin is the almost largest energy bin, including atmospheric NCQE interaction events. The final bin consists of almost only atmospheric non-NCQE type events.

The probabilities of finding the observed number of events due to the fluctuation of the background events (p-value) are evaluated for each bin to estimate how the observed events are significant over the expected data. In order to evaluate p-value, 10^6 times pseudo experiments based on the expected background events, and these systematic uncertainties are operated. The p-value is estimated using the number of events for actual observed data (N_{obs}) and for toy MC (N_{toy}) as

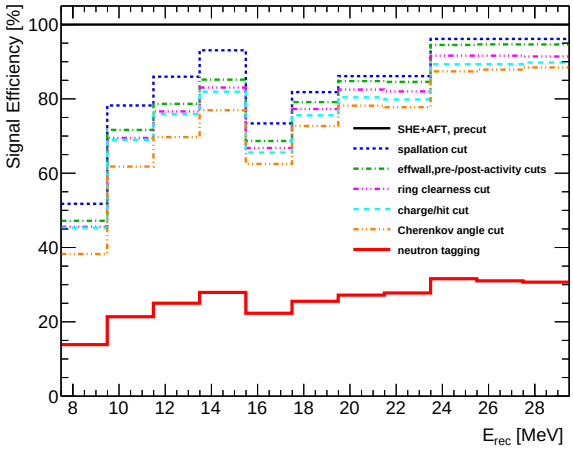

Figure 2: IBD signal efficiency for the signal energy region. The 100% efficiency line corresponds to data after noise reduction cuts. These lines show the cumulative efficiency at each cut stage, performed in the order shown in the legend. More detailed explanations for each reduction step, except for the neutron requirement, are described in Ref. [2].

follows:

$$p\text{-value} = \frac{\text{The number of toy MC with } N_{\text{toy}} \geq N_{\text{obs}}}{\text{The number of generated toy MC}}. \tag{1}$$

Table 1: Summary of observed events, expected background events, and p-value for each kinetic energy E_{rec} bin. Errors for the expected background represent only the systematic uncertainty.

E_{rec} [MeV]	Observed	Expected	p-value
7.5–9.5	5	7.73 ± 2.54	0.798
9.5–11.5	5	4.14 ± 1.23	0.398
11.5–15.5	3	2.13 ± 0.59	0.359
15.5–23.5	2	0.98 ± 0.35	0.258
23.5–29.5	1	0.98 ± 0.41	0.597

The p-value is required to be less than 0.05 for that the data implies significant excess over than expected background. Thus, we result in any significant excess that could not be found in the observed data. From this result, we extracted the 90% confidence level (C.L.) upper limit on the number of DSNB signals (N_{90}). It is evaluated by the pseudo experiments using the number of observed events with these 1σ statistical uncertainties and the number of expected background events with their systematic uncertainties. Then, the flux upper limit is calculated based on N_{90} of the observed events can be calculated as the following formula:

$$\phi_{90}^{\text{limit}} = \frac{N_{90}}{\bar{\sigma}_{\text{IBD}} \cdot N_p \cdot T \cdot \bar{\varepsilon}_{\text{sig}} \cdot dE}. \tag{2}$$

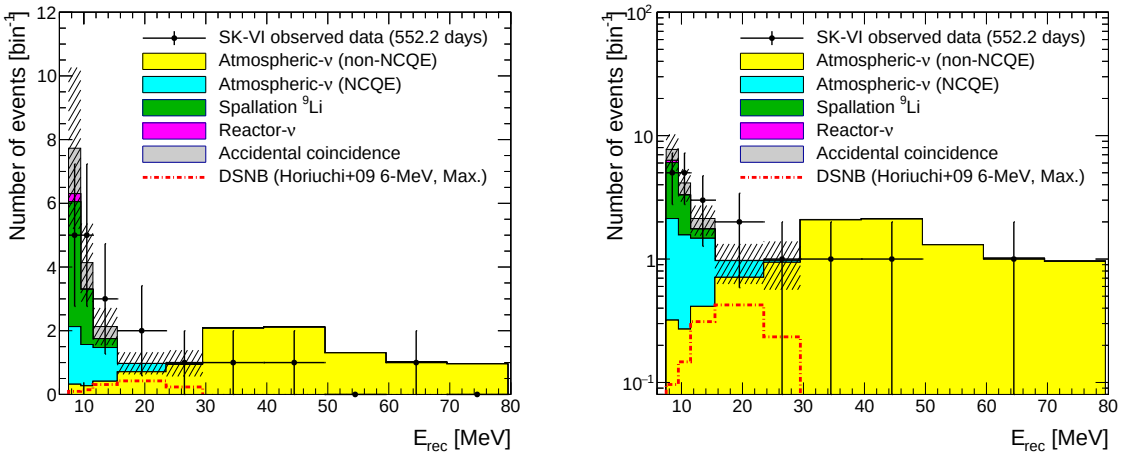

Figure 3: Reconstructed kinetic energy spectra of the observed data and expected background after data reductions with a linear (left) and a logarithmic (right) scale for the vertical axis. These include the signal energy region and the side-band region above 29.5 MeV. These color-filled background histograms are stacked on the other histograms. The error bar shown with the observed data is statistical uncertainty. The hatched areas represent the total systematic uncertainty for each energy bin. The red dotted-dashed line shows the DSNB expectation from the Horiuchi+09 model [10], which is drawn separately from the stacked histogram of the backgrounds.

Here, $\bar{\sigma}_{\rm IBD}$ is the averaged total cross-section of IBD for each energy bin, N_p is the number of protons as a target in the 22.5 ktons of the fiducial volume in SK, T is the live time of the observation (552.2 days), $\bar{\varepsilon}_{\rm sig}$ is the signal efficiency for each energy bin after all event selection criteria are applied as shown in Figure 2, and dE is the bin width at each bin. The neutrino energy E_ν is calculated by $E_\nu = E_{\rm rec} + 1.8$ MeV. The total cross-section is given by the calculation in Ref. [11]. Also, the expected upper limit from the background-only hypothesis at 90% C.L. ($N_{90}^{\rm exp}$) is evaluated using the number of expected background events and their statistical uncertainty. Then, we extract the expected flux sensitivity by replacing N_{90} with $N_{90}^{\rm exp}$ in Equation 2.

Evaluated observed upper limit and expected sensitivity on the flux are shown in Figure 4. The largest flux expectation in Figure 4 is calculated by Kaplinghat+00 model [12], and the least flux is predicted by Nakazato+15 [13] with the assumption of normal mass ordering, in whole energy ranges, respectively. Table 2 summarizes the upper limits placed by the SK at this time and previous search [2], with the range of theoretical prediction.

4. Conclusion

We report the search result for the DSNB using 552.2 days of initial data set in the SK-Gd experiment, with 0.01% Gd loaded water. This is the independent data set from the previous DSNB search [2] using pure water. The sensitivity is comparable to the previous search, though the live time is five times smaller. This is achieved by the higher neutron detection efficiency and the lowered accidental coincidence in the whole energy range. This result shows the SK-Gd experiment is the most sensitive to the DSNB in the world.

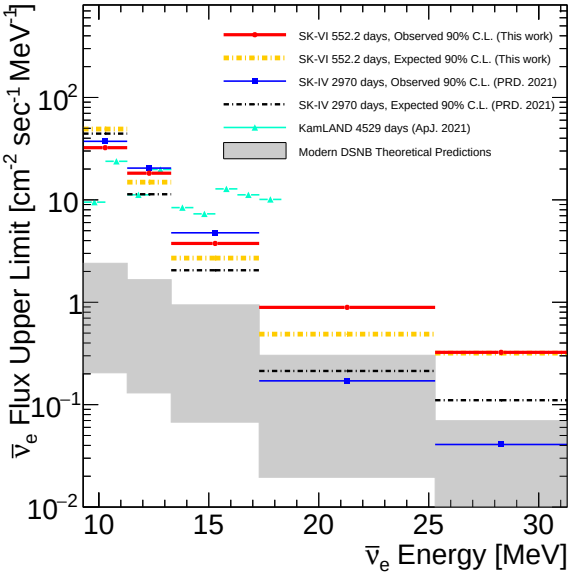

Figure 4: Upper limits on the $\bar{\nu}_e$ flux, calculated by Equation 2. The red (orange) lines show the observed (expected) 90% C.L. upper limit for SK-VI. The blue (black) lines show the observed (expected) 90% C.L. upper limit for SK-IV [2]. The cyan line represents the 90% C.L. observed upper limit placed by KamLAND [14]. The gray-shaded region represents the range of the modern theoretical expectation. The expectation drawn in the figure are for ranges of DSNB flux models of Kaplinghat+00 [12] and Nakazato+15 [13].

Table 2: Summary table of upper limits, sensitivity, and optimistic and pessimistic DSNB expectation from [12], and [13], respectively.

Neutrino Energy [MeV]	Observed upper limit [cm^{-2} s^{-1} MeV^{-1}]		Expected sensitivity [cm^{-2} s^{-1} MeV^{-1}]		Averaged theoretical expectation [cm^{-2} s^{-1} MeV^{-1}]
	SK-IV	SK-VI	SK-IV	SK-VI	
9.29–11.29	37.30	34.07	44.35	50.78	0.20 – 2.40
11.29–13.29	20.43	18.43	11.35	15.12	0.13 – 1.66
13.29–17.29	4.77	3.76	2.05	2.71	0.67 – 0.94
17.29–25.29	0.17	0.90	0.21	0.50	0.02 – 0.30
25.29–31.29	0.04	0.33	0.11	0.33	$<$ 0.01 – 0.07

References

[1] S. Fukuda, Y. Fukuda, T. Hayakawa, E. Ichihara, M. Ishitsuka, Y. Itow et al., *The Super-Kamiokande detector*, *Nuclear Instruments and Methods in Physics Research A* **501** (2003) 418.

[2] K. Abe, C. Bronner, Y. Hayato, K. Hiraide, M. Ikeda, S. Imaizumi et al., *Diffuse supernova neutrino background search at Super-Kamiokande*, *Phys. Rev. D* **104** (2021) 122002 [2109.11174].

[3] J.F. Beacom and M.R. Vagins, *Antineutrino spectroscopy with large water Čerenkov detectors*, *Phys. Rev. Lett.* **93** (2004) 171101.

[4] K. Abe, C. Bronner, Y. Hayato, K. Hiraide, M. Ikeda, S. Imaizumi et al., *First gadolinium loading to Super-Kamiokande*, *Nuclear Instruments and Methods in Physics Research A* **1027** (2022) 166248 [2109.00360].

[5] M. Harada, *Evaluation of neutron tagging efficiency for SK-Gd experiment*, *PoS* **ICHEP2022** (2022) 1178.

[6] M. Harada, *Geant4 based simulation study for super-kamiokande*, *Journal of Physics: Conference Series* **1468** (2020) 012255.

[7] S. Agostinelli, J. Allison, K. Amako et al., *Geant4—a simulation toolkit*, *Nuclear Instruments and Methods in Physics Research Section A: Accelerators, Spectrometers, Detectors and Associated Equipment* **506** (2003) 250.

[8] S.W. Li and J.F. Beacom, *First calculation of cosmic-ray muon spallation backgrounds forÂ MeV astrophysical neutrino signals in Super-Kamiokande*, *Phys. Rev. C* **89** (2014) 045801.

[9] Y. Zhang, K. Abe, Y. Haga, Y. Hayato, M. Ikeda, K. Iyogi et al., *First measurement of radioactive isotope production through cosmic-ray muon spallation in Super-Kamiokande IV*, *Phys. Rev. D* **93** (2016) 012004.

[10] S. Horiuchi, J.F. Beacom and E. Dwek, *Diffuse supernova neutrino background is detectable in Super-Kamiokande*, *Phys. Rev. D* **79** (2009) 083013 [0812.3157].

[11] A. Strumia and F. Vissani, *Precise quasielastic neutrino/nucleon cross-section*, *Physics Letters B* **564** (2003) 42 [astro-ph/0302055].

[12] M. Kaplinghat, G. Steigman and T.P. Walker, *Supernova relic neutrino background*, *Phys. Rev. D* **62** (2000) 043001 [astro-ph/9912391].

[13] K. Nakazato, E. Mochida, Y. Niino and H. Suzuki, *Spectrum of the Supernova Relic Neutrino Background and Metallicity Evolution of Galaxies*, *ApJ* **804** (2015) 75 [1503.01236].

[14] S. Abe, S. Asami, A. Gando, Y. Gando, T. Gima, A. Goto et al., *Limits on Astrophysical Antineutrinos with the KamLAND Experiment*, *ApJ* **925** (2022) 14 [2108.08527].

Full Authors List: Super-Kamiokande Collaboration

K. Abe[1,46], C. Bronner[1], Y. Hayato[1,46], K. Hiraide[1,46], K. Hosokawa[1], K. Ieki[1,46], M. Ikeda[1,46], J. Kameda[1,46], Y. Kanemura[1], R. Kaneshima[1], Y. Kashiwagi[1], Y. Kataoka[1,46], S. Miki[1], S. Mine[1,6], M. Miura[1,46], S. Moriyama[1,46], Y. Nakano[1], M. Nakahata[1,46], S. Nakayama[1,46], Y. Noguchi[1], K. Sato[1], H. Sekiya[1,46], H. Shiba[1], K. Shimizu[1], M. Shiozawa[1,46], Y. Sonoda[1], Y. Suzuki[1], A. Takeda[1,46], Y. Takemoto[1,46], H. Tanaka[1,46], T. Yano[1], S. Han[2], T. Kajita[2,46,22], K. Okumura[2,46], T. Tashiro[2], T. Tomiya[2], X. Wang[2], S. Yoshida[2], P. Fernandez[3], L. Labarga[3], N. Ospina[3], B. Zaldivar[3], B. W. Pointon[5,49], E. Kearns[4,46], J. L. Raaf[4], L. Wan[4], T. Wester[4], J. Bian[6], N. J. Griskevich[6], S. Locke[6], M. B. Smy[6,46], H. W. Sobel[6,46], V. Takhistov[6,24], A. Yankelevich[6], J. Hill[7], S. H. Lee[8], D. H. Moon[8], R. G. Park[8], B. Bodur[9], K. Scholberg[9,46], C. W. Walter[9,46], A. Beauchêne[10], O. Drapier[10], A. Giampaolo[10], Th. A. Mueller[10], A. D. Santos[10], P. Paganini[10], B. Quilain[10], T. Nakamura[11], J. S. Jang[12], L. N. Machado[13], J. G. Learned[14], K. Choi[15], N. Iovine[15], S. Cao[16], L. H. V. Anthony[17], D. Martin[17], N. W. Prouse[17], M. Scott[17], A. A. Sztuc[17], Y. Uchida[17], V. Berardi[18], M. G. Catanesi[18], E. Radicioni[18], N. F. Calabria[19], A. Langella[19], G. De Rosa[19], G. Collazuol[20], F. Iacob[20], M. Mattiazzi[20], L. Ludovici[21], M. Gonin[22], G. Pronost[22], C. Fujisawa[23], Y. Maekawa[23], Y. Nishimura[23], R. Okazaki[23], R. Akutsu[24], M. Friend[24], T. Hasegawa[24], T. Ishida[24], T. Kobayashi[24], M. Jakkapu[24], T. Matsubara[24], T. Nakadaira[24], K. Nakamura[24,46], Y. Oyama[24], K. Sakashita[24], T. Sekiguchi[24], T. Tsukamoto[24], N. Bhuiyan[25], G. T. Burton[25], F. Di Lodovico[25], J. Gao[25], A. Goldsack[25], T. Katori[25], J. Migenda[25], Z. Xie[25], S. Zsoldos[25,46], A. T. Suzuki[26], Y. Takagi[26], Y. Takeuchi[26,46], J. Feng[27], L. Feng[27], J. R. Hu[27], Z. Hu[27], T. Kikawa[27], M. Mori[27], T. Nakaya[27,46], R. A. Wendell[27,46], K. Yasutome[27], S. J. Jenkins[28], N. McCauley[28], P. Mehta[28], A. Tarant[28], Y. Fukuda[29], Y. Itow[30,31], H. Menjo[30], K. Ninomiya[30], J. Lagoda[32], S. M. Lakshmi[32], M. Mandal[32], P. Mijakowski[32], Y. S. Prabhu[32], J. Zalipska[32], M. Jia[33], J. Jiang[33], C. K. Jung[33], M. J. Wilking[33], C. Yanagisawa[33,†], M. Harada[34], Y. Hino[34], H. Ishino[34], Y. Koshio[34,46], F. Nakanishi[34], S. Sakai[34], T. Tada[34], T. Tano[34], T. Ishizuka[35], G. Barr[36], D. Barrow[36], L. Cook[36,46], S. Samani[36], D. Wark[36,41], A. Holin[37], F. Nova[37], B. S. Yang[38], J. Y. Yang[38], J. Yoo[38], J. E. P. Fannon[39], L. Kneale[39], M. Malek[39], J. M. McElwee[39], M. D. Thiesse[39], L. F. Thompson[39], S. T. Wilson[39], H. Okazawa[40], S. B. Kim[42], E. Kwon[42], J. W. Seo[42], I. Yu[42], A. K. Ichikawa[43], K. D. Nakamura[43], S. Tairafune[43], K. Nishijima[44], A. Eguchi[45], K. Nakagiri[45], Y. Nakajima[45,46], S. Shima[45], N. Taniuchi[45], E. Watanabe[45], M. Yokoyama[45,46], P. de Perio[46], S. Fujita[46], K. Martens[46], K. M. Tsui[46], M. R. Vagins[46,6], J. Xia[46], S. Izumiyama[47], M. Kuze[47], R. Matsumoto[47], M. Ishitsuka[48], H. Ito[48], Y. Ommura[48], N. Shigeta[48], M. Shinoki[48], K. Yamauchi[48], T. Yoshida[48], R. Gaur[49], V. Gousy-Leblanc[49,‡], M. Hartz[49], A. Konaka[49], X. Li[49], S. Chen[50], B. D. Xu[50], B. Zhang[50], M. Posiadala-Zezula[51], S. B. Boyd[52], R. Edwards[52], D. Hadley[52], M. Nicholson[52], M. O'Flaherty[52], B. Richards[52], A. Ali[53,49], B. Jamieson[53], S. Amanai[54], Ll. Marti[54], A. Minamino[54], and S. Suzuki[54]

[1]Kamioka Observatory, Institute for Cosmic Ray Research, University of Tokyo, Kamioka, Gifu 506-1205, Japan
[2]Research Center for Cosmic Neutrinos, Institute for Cosmic Ray Research, University of Tokyo, Kashiwa, Chiba 277-8582, Japan
[3]Department of Theoretical Physics, University Autonoma Madrid, 28049 Madrid, Spain
[4]Department of Physics, Boston University, Boston, MA 02215, USA
[5]Department of Physics, British Columbia Institute of Technology, Burnaby, BC, V5G 3H2, Canada
[6]Department of Physics and Astronomy, University of California, Irvine, Irvine, CA 92697-4575, USA
[7]Department of Physics, California State University, Dominguez Hills, Carson, CA 90747, USA
[8]Institute for Universe and Elementary Particles, Chonnam National University, Gwangju 61186, Korea
[9]Department of Physics, Duke University, Durham NC 27708, USA
[10]Ecole Polytechnique, IN2P3-CNRS, Laboratoire Leprince-Ringuet, F-91120 Palaiseau, France
[11]Department of Physics, Gifu University, Gifu, Gifu 501-1193, Japan
[12]GIST College, Gwangju Institute of Science and Technology, Gwangju 500-712, Korea
[13]School of Physics and Astronomy, University of Glasgow, Glasgow, Scotland, G12 8QQ, United Kingdom
[14]Department of Physics and Astronomy, University of Hawaii, Honolulu, HI 96822, USA
[15]Institute for Basic Science (IBS), Daejeon, 34126, Korea
[16]Institute For Interdisciplinary Research in Science and Education, ICISE, Quy Nhon, 55121, Vietnam
[17]Department of Physics, Imperial College London , London, SW7 2AZ, United Kingdom
[18]Dipartimento Interuniversitario di Fisica, INFN Sezione di Bari and Università e Politecnico di Bari, I-70125, Bari, Italy
[19]Dipartimento di Fisica, INFN Sezione di Napoli and Università di Napoli, I-80126, Napoli, Italy
[20]Dipartimento di Fisica, INFN Sezione di Padova and Università di Padova, I-35131, Padova, Italy
[21]INFN Sezione di Roma and Università di Roma "La Sapienza", I-00185, Roma, Italy
[22]ILANCE, CNRS - University of Tokyo International Research Laboratory, Kashiwa, Chiba 277-8582, Japan
[23]Department of Physics, Keio University, Yokohama, Kanagawa, 223-8522, Japan
[24]High Energy Accelerator Research Organization (KEK), Tsukuba, Ibaraki 305-0801, Japan
[25]Department of Physics, King's College London, London, WC2R 2LS, UK
[26]Department of Physics, Kobe University, Kobe, Hyogo 657-8501, Japan
[27]Department of Physics, Kyoto University, Kyoto, Kyoto 606-8502, Japan
[28]Department of Physics, University of Liverpool, Liverpool, L69 7ZE, United Kingdom
[29]Department of Physics, Miyagi University of Education, Sendai, Miyagi 980-0845, Japan
[30]Institute for Space-Earth Environmental Research, Nagoya University, Nagoya, Aichi 464-8602, Japan
[31]Kobayashi-Maskawa Institute for the Origin of Particles and the Universe, Nagoya University, Nagoya, Aichi 464-8602, Japan
[32]National Centre For Nuclear Research, 02-093 Warsaw, Poland
[33]Department of Physics and Astronomy, State University of New York at Stony Brook, NY 11794-3800, USA
[34]Department of Physics, Okayama University, Okayama, Okayama 700-8530, Japan
[35]Media Communication Center, Osaka Electro-Communication University, Neyagawa, Osaka, 572-8530, Japan
[36]Department of Physics, Oxford University, Oxford, OX1 3PU, United Kingdom
[37]Rutherford Appleton Laboratory, Harwell, Oxford, OX11 0QX, UK
[38]Department of Physics, Seoul National University, Seoul 151-742, Korea

[†]also at BMCC/CUNY, Science Department, New York, New York, 1007, USA.

[‡]also at University of Victoria, Department of Physics and Astronomy, PO Box 1700 STN CSC, Victoria, BC V8W 2Y2, Canada.

[39]Department of Physics and Astronomy, University of Sheffield, S3 7RH, Sheffield, United Kingdom
[40]Department of Informatics in Social Welfare, Shizuoka University of Welfare, Yaizu, Shizuoka, 425-8611, Japan
[41]STFC, Rutherford Appleton Laboratory, Harwell Oxford, and Daresbury Laboratory, Warrington, OX11 0QX, United Kingdom
[42]Department of Physics, Sungkyunkwan University, Suwon 440-746, Korea
[43]Department of Physics, Faculty of Science, Tohoku University, Sendai, Miyagi, 980-8578, Japan
[44]Department of Physics, Tokai University, Hiratsuka, Kanagawa 259-1292, Japan
[45]Department of Physics, University of Tokyo, Bunkyo, Tokyo 113-0033, Japan
[46]Kavli Institute for the Physics and Mathematics of the Universe (WPI), The University of Tokyo Institutes for Advanced Study, University of Tokyo, Kashiwa, Chiba 277-8583, Japan
[47]Department of Physics,Tokyo Institute of Technology, Meguro, Tokyo 152-8551, Japan
[48]Department of Physics, Faculty of Science and Technology, Tokyo University of Science, Noda, Chiba 278-8510, Japan
[49]TRIUMF, 4004 Wesbrook Mall, Vancouver, BC, V6T2A3, Canada
[50]Department of Engineering Physics, Tsinghua University, Beijing, 100084, China
[51]Faculty of Physics, University of Warsaw, Warsaw, 02-093, Poland
[52]Department of Physics, University of Warwick, Coventry, CV4 7AL, UK
[53]Department of Physics, University of Winnipeg, MB R3J 3L8, Canada
[54]Department of Physics, Yokohama National University, Yokohama, Kanagawa, 240-8501, Japan